Study of Receptor-Chaperone Interactions Using the Optical Technique of Spectroscopic Ellipsometry

Verena Kriechbaumer,[†*] Anna Tsargorodskaya,[‡] Mohd K. Mustafa,[‡] Tatiana Vinogradova,[‡] Joanne Lacey,[†] David P. Smith,[†] Benjamin M. Abell,[†] and Alexei Nabok[‡]
[†]Biomedical Research Centre and [‡]Materials and Engineering Research Institute, Sheffield Hallam University, Sheffield, United Kingdom

ABSTRACT This work describes a detailed quantitative interaction study between the novel plastidial chaperone receptor OEP61 and isoforms of the chaperone types Hsp70 and Hsp90 using the optical method of total internal reflection ellipsometry (TIRE). The receptor OEP61 was electrostatically immobilized on a gold surface via an intermediate layer of polycations. The TIRE measurements allowed the evaluation of thickness changes in the adsorbed molecular layers as a result of chaperone binding to receptor proteins. Hsp70 chaperone isoforms but not Hsp90 were shown to be capable of binding OEP61. Dynamic TIRE measurements were carried out to evaluate the affinity constants of the above reactions and resulted in clear discrimination between specific and nonspecific binding of chaperones as well as differences in binding properties between the highly similar Hsp70 isoforms.

INTRODUCTION

The optical method of spectroscopic ellipsometry in its total internal reflection version, i.e., total internal reflection ellipsometry (TIRE), has been developed for the analysis of interactions between antibodies and various ligands (1–3), particularly for detection of low-molecular-weight analytes such as pesticides (4), mycotoxins (1,4–6), and alkylphenols (7) but other types of protein-protein interactions have not been tested. TIRE—a combination of spectroscopic ellipsometry and surface plasmon resonance (SPR)—offers 10-times better sensitivity than conventional SPR (1,8) and provides high sensitivity in the detection of affinity reactions.

Our biological interest is to use TIRE to study receptor-protein interactions, with the potential to analyze such interactions at native membrane surfaces. Physical methods such as TIRE can complement traditional biological methods of studying protein-protein interaction and provide necessary quantification of such interactions. Another key element of this work is the use of electrostatic immobilization of proteins via an intermediate polycation layer of polyallylamine hydrochloride (PAH) (9). This technology proved to be universal and was widely used for immobilization of different biomolecules, i.e., enzymes (10,11), antibodies (1,2,4–6), or DNA (4), on solid surfaces.

This study investigates the role that different chaperone types and isoforms play in targeting specificity. The binding behavior and binding affinities of the novel plant chaperone receptor OEP61 (outer envelope protein of 61 kDa) toward the various chaperone types and isoforms was investigated using the method of TIRE as primary detection technique. OEP61 is ideal for testing differences in binding affinity between closely related chaperone isoforms that are highly similar in amino-acid sequence. This will allow us to show the discriminatory powers of the TIRE method.

Chaperone proteins help cells to deal with high temperatures and other cellular stresses; they stabilize protein structures, prevent protein aggregation, or degrade misfolded proteins. Furthermore, most protein targeting pathways are dependent upon cytosolic molecular chaperones and freshly translated proteins are often in a complex with cytosolic molecular chaperones (12) such as heat shock protein70 (Hsp70) or heat shock protein90 (Hsp90). Current models suggest that chaperones simply prevent precursor protein aggregation, but there is growing evidence supporting the notion that they also determine the specificity of targeting. The recent finding of chaperone receptors in plants, like Toc64 at the chloroplast membrane (13) and mtOM64 (14) at the mitochondrial membrane, indicates a more specific involvement of molecular chaperones in protein targeting. These receptors feature tetratricopeptide repeat (TPR) domains able to specifically bind the highly conserved C-terminus of Hsp70 and/or Hsp90. The C-terminal pentapeptide MEEVD of Hsp90 is essential and sufficient for TPR domain binding while the binding of Hsp70 to TPR domains depends on the C-terminal heptapeptide (PTIEEVD in mammals, PKIEEVD in plants) (15–17). The binding of Hsp70 was shown to be more specific than the binding of Hsp90 (18,16).

Interestingly, at least one of these chaperone receptors can be found on each organelle (19), which suggests a universal role in protein targeting for these chaperone receptors (for review, see (20)). Chaperones might provide specificity to the targeting process by recognizing features of the bound protein they deliver, and form unique signatures through distinct combinations of chaperones which are then recognized by membrane receptors at the destination organelle.

Submitted May 10, 2011, and accepted for publication June 9, 2011.

*Correspondence: v.kriechbaumer@shu.ac.uk

Editor: Doug Barrick.

0006-3495/11/07/0504/8 $2.00

doi: 10.1016/j.bpj.2011.06.011

The molecular chaperone Hsp70 has been shown to play an important role in protein targeting to ER (21) and mitochondria (22), and membrane-localized proteins destined for chloroplasts are delivered to Toc64 by Hsp90 (13), yet the function of chaperones in defining localization or targeting specificity is unknown. *Arabidopsis* possesses at least eighteen distinct Hsp70 proteins (23), five of them cytosolic (24,25) and seven Hsp90 proteins (26).

The novel chaperone receptor used in this protein interaction study—OEP61—was recently identified in a bioinformatics search based on the structural alignment of known chaperone receptors and their characteristic TPR region clamp domain. OEP61 was shown to be localized at the chloroplast outer envelope in *Arabidopsis thaliana* anchored into the membrane by its C-terminal end with the rest of the protein facing the cytosol. OEP61 is able to bind specifically to Hsp70 chaperones as well as to precursor protein complexes destined for chloroplasts via its TPR domain. Addition of nonmembrane-bound OEP61 lacking its transmembrane (TM) domain represses the chloroplast import of the plastidial protein Toc33 severely (27). These data strongly indicate that OEP61 functions as chaperone receptor.

This study investigates the role that different chaperone types and isoforms play in targeting specificity and the method of TIRE is utilized here as a useful and highly sensitive technique to study the affinity of chaperone-receptor interaction.

The parameters of the effective thickness of the adsorbed molecular layer (obtained from single spectroscopic TIRE measurements) and the affinity constant (obtained from dynamic TIRE measurements) gave valuable quantitative information about the mechanism of chaperone-receptor interaction. A clear distinction between specific and nonspecific interaction is reported for the first time, to our knowledge.

SAMPLE PREPARATION AND EXPERIMENTAL METHODS

Heterologous protein expression and purification

Clones for Hsp70-1 (At5g02500), Hsp70-2 (At5g02490), Hsp70b (At1g16030), Hsp90-2 (At5g56030), OEP61 (At5g21990), and Toc64 (At3g17970) were obtained as cDNAs in plasmids from The *Arabidopsis* Information Resource (TAIR, Stanford, CA). The coding sequence for Hsp90-4 (At5g56000) was amplified from cDNA using the following primer combinations introducing *Nde*I and *BamH*I restriction sites, respectively:

Hsp90-4forward: CTTTGGCAGATCTACCCATATGGCGGACGCAGAG,
Hsp90-4reverse: TAAAGGATCCTTAGTCGACTTCCTC.

The coding regions of the chaperone isoforms and the chaperone receptors were cloned into a pET16b expression vector containing a 6-His-tag (Novagen, Madison, WI) and proteins were heterologously expressed in T7 Express *Iq Escherichia coli* cells (New England Biolabs, Ipswich, MA). To allow soluble expression of the membrane-bound receptors OEP61 and Toc64 in sufficient amounts, the hydrophobic TM domains were removed using the following primer combinations (restriction sites are given in brackets):

OEP61-TMforward: ATATCTCGAGTTTAACGGGTTAATGGATCC (*Xho*I),
OEP61-TMreverse: ATATAGATCTTTATTTTCCGAACAACCACTTC (*Bgl*II),
Toc64-TMforward ATATCATATGGATCCAAACACCCTACGTCG (*Nde*I),
Toc64-TMreverse: TAAA GGATCCTCACTGGAATTTTCTCAGTC (*BamH*I).

Plasmids containing the coding sequence for Hop1 and Hop2A were kindly donated by Dr. Jason Young (McGill University, Montreal, Quebec, Canada).

Bacterial cells were harvested by centrifugation at 8000 × *g* for 8 min, resuspended in lysis buffer (50 mM NaH_2PO4, 300 mM NaCl, 10 mM imidazole, pH8.0), and treated with lysozyme (1 mg/ml) for 30 min on ice. The resulting lysate was sonicated three times at 200 W for 10 s and was centrifuged at 10,000 × *g* for 30 min at 4°C. His-tagged proteins were purified under native conditions using Ni-NTA agarose according to the manufacturer's manual (Qiagen, Venlo, The Netherlands). Dialysis against 50 mM Tris-HCl, pH 8.0, and His-tag cleavage were performed.

Pulldown assays

His-tagged OEP61, Hop1, and PEX19 proteins were expressed in T7 Express *Iq E. coli* cells (New England Biolabs), and purified by chromatography on Ni-NTA agarose (Promega, Madison, WI). Pulldown experiments from rabbit reticulocyte lysate (RRL) were performed according to Young et al. (28) with the following changes: 1 μM His-tagged protein was linked to Ni-NTA agarose in buffer CG (100 mM KOAc, 20 mM HEPES-KOH (pH 7.5), 5 mM $MgOAc_2$) containing 2 mg/ml ovalbumin and 0.1% Triton X-100. Agarose-bound recombinant proteins were incubated in buffer CG containing 2 mg/ml ovalbumin, 0.1% Triton X-100, and 25% RRL for 2 h. Washes with buffer CG containing 0.1% Triton X-100 were performed. Finally, the Ni-NTA agarose was heated in protein loading buffer at 70° for 10 min and the resulting supernatant analyzed by sodium dodecyl sulfate-polyacrylamide gel electrophoresis (SDS-PAGE).

Western blotting

For Western blotting, proteins were transferred from SDS-PAGE gels to PVDF membranes (Millipore, Billerica, MA) according to the manufacturer's instructions. Primary anti-human Hsp70 IgG (Stratagene, La Jolla, CA) were used at 1:10,000 and secondary goat anti-rabbit IgG labeled with Alexa Fluor 594 dye (Invitrogen, Carlsbad, CA) were used at 1:3000. Signals were detected using the ODYSSEY Infrared imaging system (LI-COR Biosciences, Lincoln, NE).

Immobilization of receptors on solid surfaces

The substrates for TIRE study were prepared by thermal evaporation of gold onto microscopic glass slides. Typical thickness of gold layer was 25–27 nm, which was monitored by quartz crystal microbalance sensor. To improve adhesion of gold layer to the surface, a thin (2–3 nm) layer of chromium was deposited first. Deposition of both metals was carried out using an Edwards A360 metallization unit (Edwards Lifesciences, Irvine, CA) without breaking the vacuum of ~10^{-6} Torr.

The gold-coated glass slides produced can be used for electrostatic deposition of proteins as they are; however, the negative surface charge can be enhanced by treating the slides overnight in 0.1 M solution of mercapto-ethylsulfonate sodium salt $SH\text{-}(CH_2)_2\text{-}SO_3^-\ Na^+$ in methanol. The

immobilization of proteins on the gold surface was achieved by positively charging the surface with polyallylamine hydrochloride (PAH, 2 mg/ml). An incubation time of 15 min was sufficient to achieve saturation of PAH adsorption. The sample was then rinsed by purging the cell with 10-times the cell volumes of deionized water. After that, the surface is ready for electrostatic adsorption of proteins, which are typically negatively charged in slightly alkaline (pH 8.0) Tris-HCl buffer solution.

TIRE experiments

TIRE measurements were performed using the experimental setup described previously in detail (1,4–6). It is based on a J. A. Woollam (Lincoln, NE) spectroscopic ellipsometer M2000 operating in the spectral range of 370–1000 nm, and exploiting the rotating compensator principle. The additional element in TIRE is a 68° trapezoidal glass prism through which the light is coupled into thin metal (Au) film deposited on a glass slide. Index matching fluid is used for optical contact between the prism and glass slide. The reaction cell with the volume of 0.2 ml is positioned underneath the gold layer. The inlet and outlet tubes allow the injection of required solutions into the cell to perform adsorption of different molecules on the surface. A typical sequence of adsorption steps used in this work was 1), PAH (2 mg/ml aqueous solution), 2), receptor proteins (10 μg/ml solution in 100 mM Tris-HCl, pH 8.0), and 3), chaperones in increasing concentrations (in 100 mM Tris-HCl, pH 8.0) with 15-min incubation time.

Rinsing the cell was carried out after every deposition step by purging 10-times the cell volume with 100 mM Tris-HCl, pH 8.0, solution.

Spectroscopic ellipsometry provides the spectra of two ellipsometric parameters Ψ and Δ, which are, respectively, related to the ratio of the amplitudes and the phase shift of p- and s-components of polarized light. Actually, the ability of recording spectra of phase-related parameter Δ distinguishes the method of TIRE from conventional SPR. The parameter Δ is 10-times more sensitive than Ψ to small changes in the optical density of adsorbed molecular layers (1), which constitutes the main advantage of using TIRE. It was shown that the phase-sensitive TIRE method offers 10-times higher sensitivity than the conventional SPR method based on the detection of the intensity of reflected light (1,8).

Two types of ellipsometric measurements were performed: 1), dynamic TIRE spectral measurements, i.e., a number of TIRE spectra recorded after a certain time interval during every adsorption (or binding) step, and 2), TIRE single spectra scans, which were recorded after completion of every adsorption step in a standard buffer solution (pH 8.0).

The dynamic TIRE spectra are recorded in situ, i.e., in the course of molecular adsorption (or binding). Because the refractive index of injected solutions may vary, the evaluation of the thickness and optical constants of molecular layer is not strictly correct. Dynamic TIRE measurements can be used, however, for the analysis of the kinetics of adsorption or binding reactions. Single spectra scans performed in the same buffer solution in steady-state conditions (after completion of adsorption) were thus suitable for TIRE data fitting.

Software provided by J. A. Woollam (29) allowed the modeling of the reflection system and subsequent evaluation of the thickness and refractive index of adsorbed molecular layer by comparing the experimental and theoretical values of Ψ and Δ and minimizing the error function. A four-layer model, typically used in our TIRE measurements, is shown in Table 1. The thickness (d) and complex refractive index (n-ik) dispersion for gold layer was evaluated first by fitting TIRE spectra recorded on bare gold surface; then the obtained parameters were kept fixed during further fittings on the same sample. A principle limitation of the ellipsometry and SPR methods is that the simultaneous evaluation of d and n of thin ($<$10 nm) dielectric films is impossible (either one or another parameter must be fixed during fitting). In our work, we keep the refractive index fixed and associate all the changes in the adsorbed layer with the thickness. This is not strictly correct, but more close to reality because all bioorganic substances have similar refractive indices of ~1.42 (at 633 nm) (30).

RESULTS AND DISCUSSION

OEP61 pulldown experiments

To test which chaperone types interact with OEP61, conventional pulldown assays were performed using recombinantly expressed His-tagged OEP61 and RRL (Fig. 1 *A*, lane *1* with RRL). Ni-beads bind the His-tag of OEP61 and thereby precipitate any proteins complexed with OEP61.

These binding experiments were controlled using the extensively studied mammalian Hsp70 and Hsp90 organizing protein (Hop (31)). Like OEP61, Hop is a TPR clamp protein able to bind chaperones. The N-terminal fragment of Hop (Hop1) is known to bind Hsp70 and the C-terminal fragment (Hop2A) binds Hsp90. The ability of Hop to bind both Hsp70 and Hsp90 makes it a model TPR-containing protein for studying chaperone-TPR domain binding. As negative controls, pulldowns were also performed with Ni-beads only and an unrelated His-tagged protein (PEX19).

OEP61 forms a protein complex with Hsp70, but does not show binding to Hsp90 chaperones (Fig. 1 *A*, lane *6*). Both positive controls Hop1 (lane *4*) and Hop2A (lane *5*) bind Hsp70 and Hsp90, respectively, and the negative controls of Ni-beads and PEX19 (lanes *2* and *3*) bind neither Hsp70 nor Hsp90.

In this experiment, Hop2A also interacts with Hsp70, although to a lower extent than with Hsp90. This is consistent with previous studies showing that Hop2A is able to bind Hsp70 with a low affinity whereas Hop1 does not bind Hsp90 at all, indicating that the binding of Hsp70 is more specific than the binding of Hsp90 (18,16).

Immunoblots probed with anti-Hsp70 antibodies (Fig. 1 *B*) confirm that the band present in pulldowns with OEP61 (lane *3*) and Hop1 (lane *2*) but not in the negative control PEX19 (lane *1*) is indeed Hsp70.

TIRE: differentiation of specific and nonspecific binding

As pulldown experiments cannot distinguish between the binding affinities of highly similar chaperone isoforms, TIRE analysis with recombinantly expressed chaperones and receptors was performed. TIRE spectra $\Delta(\lambda)$ are recorded in a steady-state manner after consecutive adsorption of layers of PAH, OEP61 receptor proteins, and chaperone proteins in progressively increasing concentrations. Fitting these TIRE spectra allows the evaluation of the thicknesses of all adsorbed layers. The resolution of the obtained thickness values is in the range of 0.01 nm, which is sufficient to record the response of chaperone binding at concentrations as low as 1 ng/ml. The resulting calibration curves for three different Hsp70 isoforms binding to OEP61 are shown in Fig. 2.

A common feature in these curves is the saturation of the response at medium concentrations of chaperones at ~1 μg/ml followed by a sharp increase of the response at

TABLE 1 The four-layer model for TIRE data fitting

Layer	Parameters	Comments
3. BK33-7 glass (ambient)	n, k dispersions from WVASE32 library, $n = 1.515$, $k = 0$ at 633 nm.	Fixed during fitting.
2. Cr/Au film	$n = 0.359 \pm 0.078$; $k = 2.857 \pm 0.114$ at 633 nm. d is varied in the range of 25–30 nm.	The values of d, and dispersions for n and k were obtained by fitting TIRE data for every new sample, then kept fixed in further fittings.
1. Adsorbed layer	Cauchy model: $n = A + \frac{B}{\lambda^2} + \frac{C}{\lambda^4}$, where $A = 1.396$, $B = 0.01$, $C = 0$, giving $n = 1.42$, $k = 0$ at 633 nm.	Parameters of Cauchy model A, B, and C are fixed; d is variable.
0. Water (substrate)	n, k dispersions from WVASE32 library, $n = 1.33$, $k = 0$, at 633 nm.	Fixed during fitting.

higher concentrations. This response at high concentration of chaperones (above 1 μg/ml) is likely to be caused by nonspecific binding. This is feasible considering that the OEP61 receptors were immobilized on the surface from a 10 μg/ml solution, so chaperone concentrations higher than that value are most likely causing nonspecific binding (i.e., more than one chaperone molecule per molecule of receptor). However, the chaperone-receptor ratio on a sample surface could be different from that in solution and the critical concentration could be smaller than 10 μg/ml. More detailed analysis is therefore required.

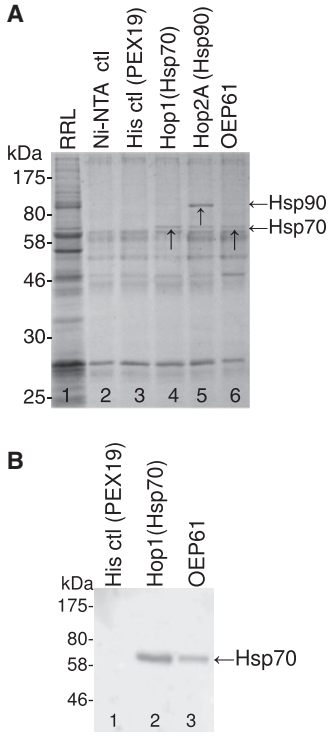

FIGURE 1 Interaction between OEP61 and chaperones in RRL. (*A*) OEP61 was incubated with RRL and isolated by its His-tag. The resulting binding partners were analyzed by SDS-PAGE and Coomassie staining (lane *6*). The Hsp70- or Hsp90-binding fragment of Hop (Hop1 and Hop2A, lanes *4* and *5*), respectively, were used as positive controls. Pulldown assays with Ni-NTA agarose only (lane *2*) and an unrelated His-tagged protein (PEX19, lane *3*) were used as negative controls. (*B*) Immunoblotting with anti-Hsp70 antibodies was performed for the pulldown assays with OEP61 (lane *3*) and the Hsp70-binding fragment of Hop (Hop1, lane *2*). His-tagged PEX19 was used as a negative control (lane *1*).

The reaction between receptors and chaperone is considered to be a simple model of binding target molecules (chaperones) to single binding sites (receptors) on the surface, which is described by the differential equation (32)

$$\frac{dn}{dt} = k_a C(N - n) - k_d n, \tag{1}$$

where $k_a(\mathrm{Mol}^{-1}\ \mathrm{s}^{-1})$, $k_d(\mathrm{s}^{-1})$ are adsorption and desorption rates, respectively. Note that C(Mol) is the concentration of analyte (i.e., chaperone) in the environment (solution), $(\mathrm{Mol}\cdot\mathrm{m}^{-2})$ is the concentration of adsorbed analyte on the surface, and $\mathrm{N}(\mathrm{Mol}\cdot\mathrm{m}^{-2})$ is the concentration of binding sites (i.e., receptor) on the surface. Consequently, N–n is the concentration of available binding sites on the surface. The solution of this equation is given as (33):

$$n = N\frac{k_a C}{k_a C + k_d}\left[1 - e^{-(k_a C + k_d)t}\right]. \tag{2}$$

At saturation, when $x \to \infty$, it transforms into

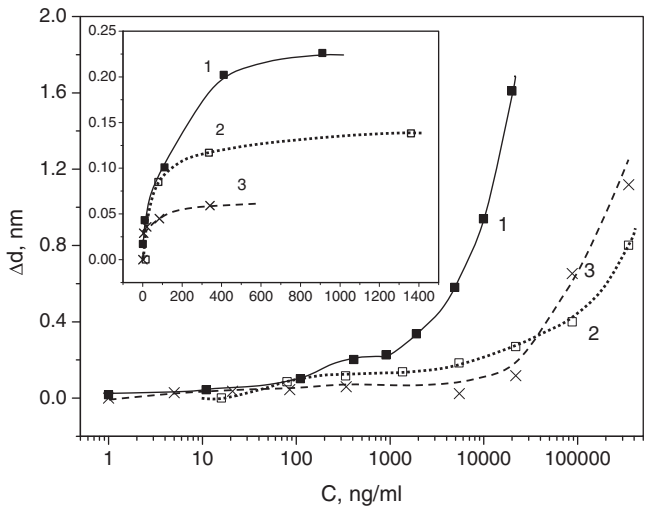

FIGURE 2 Calibration curves (e.g., thickness increment versus chaperone concentration) for binding chaperones Hsp70-1 (*1*), Hsp70-2 (*2*), and Hsp70b (*3*) to OEP61 receptors immobilized on a gold surface. (*Inset*) Section of calibration curves at low chaperone concentrations in a linear scale with the same units as in the main figure.

$$n = N\frac{k_aC}{k_aC + k_d} = \frac{N}{1 + \frac{k_d}{k_aC}}. \quad (3)$$

After transformation, one can obtain that if the concentration (C) is high, $n \approx N$, whereas for small C values, $n \approx CNk_a/k_d = CNK_A$, where $K_A(\mathrm{Mol}^{-1}) = k_a/k_d$ is the association constant, which is also reciprocal to the affinity constant $K_A = 1/K_D$.

In our case of receptor-chaperone interaction, the concentration of receptors on the surface (at saturation) can be presented as

$$n_R \approx NC_RK_A^R, \quad (4)$$

where N is the concentration of binding sites on the surface, C_R is the concentration of receptors in solution, and $K^R{}_A$ is the association constant for receptors. The concentration of target molecules (chaperones) bound to receptors is

$$n_T \approx n_RC_TK_A^T = NC_RC_TK_A^RK_A^T, \quad (5)$$

where C_T is the concentration of target molecules in solution and $K^T{}_A$ is the association constant for target molecules on receptors. Therefore, the target/receptor ratio on the surface is

$$\frac{n_T}{n_R} = C_TK_A^T. \quad (6)$$

To find out the concentration of target molecules in solution which is required to achieve full saturation of binding sites, i.e., $n_T = n_R$, the following transformations have to be made, i.e.,

$$1 = \frac{n_T}{n_R} = C_TK_A^T = \frac{C_T(\mathrm{g/L}) \times K_A^T(\mathrm{L/mol})}{M_T(\mathrm{g/mol})}, \quad (7)$$

where M_T is the molecular mass.

For example, for the receptor OEP61 binding Hsp70 chaperones, the association constant is in the range of $K^T{}_A = 6.11 \times 10^8$ (mol/l). With a molecular mass for Hsp70 chaperones of $M_T = 7 \times 10^4$ (g/mol), it can be estimated as $C_T = 1.15 \cdot 10^{-4}(\mathrm{g/L}) = 0.115(\mathrm{mg/L}) = 0.115(\mu\mathrm{g/mL})$. This value should be tripled to account for random orientation of receptors electrostatically adsorbed on the surface. The obtained value of ~0.2 μg/ml corresponds well to the observed transition from specific to nonspecific binding in TIRE measurements (Fig. 2).

The equilibrium point between receptor and target molecules on the surface is shifted to the lower concentrations in comparison to the equilibrium in the solution at $C_T = C_R = 10(\mu\mathrm{g/ml})$. Such a trend was observed for all chaperone/receptor pairs studied.

A clear mathematical distinction between specific and nonspecific interaction fits with the experimentally observed binding behavior and allows the evaluation of critical chaperone concentrations of chaperone, outlining the border between specific and nonspecific interaction.

TIRE steady-state measurements

TIRE steady-state spectra showed that OEP61 is capable of binding all three tested Hsp70 isoforms. However, the different isoforms feature different response curves with the receptor (Fig. 2). Binding of Hsp70-1 is the most efficient of the Hsp70 isoforms tested because it shows the largest response, with binding starting already from concentrations below 1 ng/ml and with a saturation at ~1 μg/ml (Fig. 2, curve *1*). Hsp70-2 demonstrates binding only above 20 ng/ml with saturation at ~0.5 μg/ml (Fig. 2, curve *2*) and therefore half the saturation of Hsp70-1. Binding of Hsp70b starts at ~5 ng/ml but the saturation is three-times lower than for the Hsp70-1 with 350 ng/ml (Fig. 2, curve *3*). Interestingly and confirming the pulldown data, OEP61 did not bind any of the tested Hsp90 chaperone isoforms indicating a distinct OEP61 binding specificity differentiating between the Hsp70 and Hsp90 chaperone type (exemplified for Hsp90-2, Fig. 3, curve *3*).

To test for general functionality of the recombinant chaperones, especially for the nonbinding Hsp90 isoforms, these binding experiments were controlled using the Hsp70-binding Hop1 fragment and the Hsp90-binding Hop2A fragment (32). Furthermore, because Hop is a mammalian protein and might therefore have a different binding behavior toward plant chaperones, a well-characterized plant plastidial chaperone receptor Toc64—known to bind Hsp90 via its TPR domain (13)—was also included in this study to test for Hsp90 functionality.

Hop1 responds with the tested Hsp70 isoforms, Hsp70-1 and Hsp70b, in a similar manner as OEP61 (Fig. 4, *A* and *B*) and both Hsp90-controls, Hop2A and Toc64,

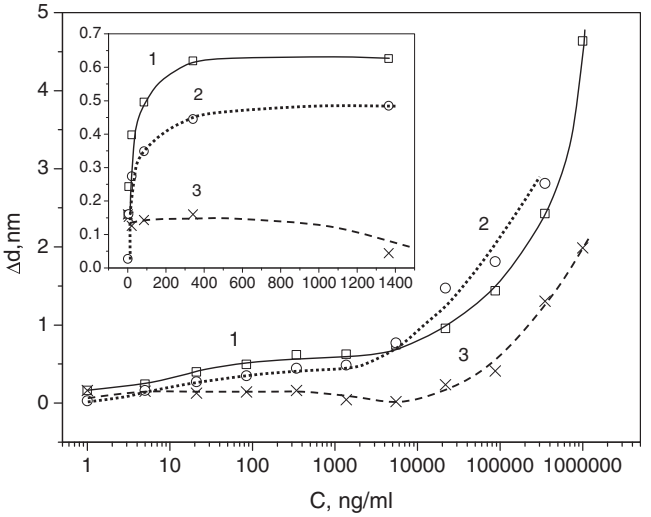

FIGURE 3 Calibration curves (e.g., thickness increment versus chaperone concentration) for binding Hsp90 chaperones to the Hsp90 binding Hop fragment Hop2A (*1*) and the plastidial chaperone receptor Toc64 (*2*) as positive controls and OEP61 (*3*). (*Inset*) Section of calibration curves at low chaperone concentrations in a linear scale with the same units as in the main figure.

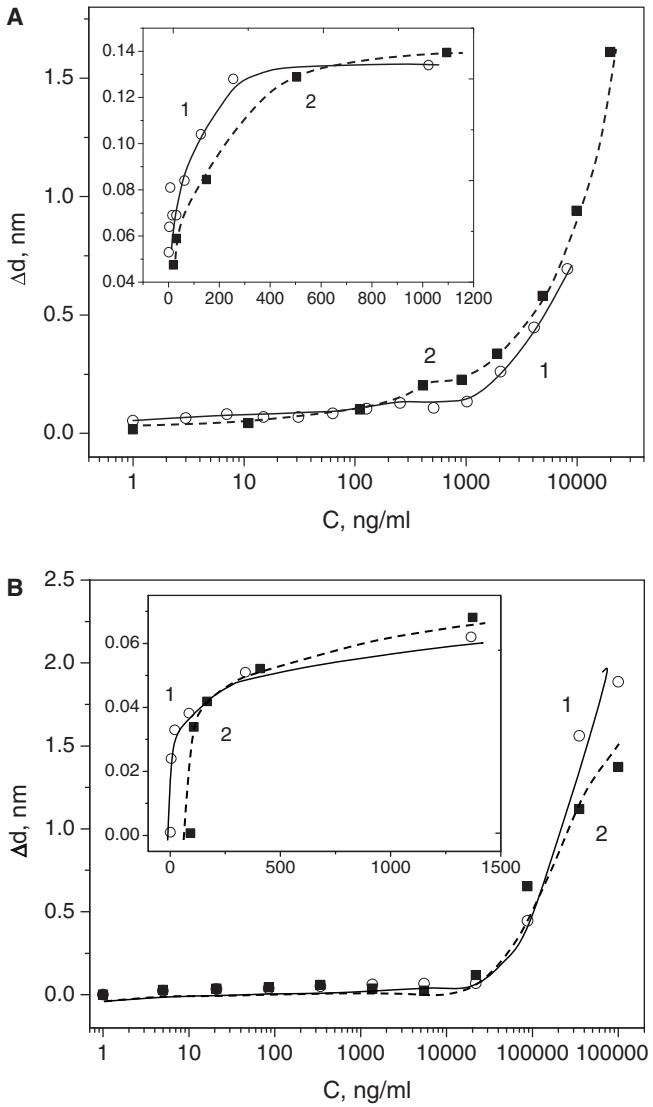

FIGURE 4 Calibration curves (e.g., thickness increment versus chaperone concentration) for the binding of chaperones Hsp70-1 (*A*) and Hsp70b (*B*) to the positive control Hop1 (curve *1*) and the receptor OEP61 (curve *2*) immobilized on a gold surface. (*Inset*) Section of calibration curves at low chaperone concentrations in a linear scale with the same units as in the main figure.

bind the Hsp90 isoforms efficiently, showing functionality of the recombinantly expressed proteins (Fig. 3, curves *1* and *2*).

TIRE dynamic spectral measurements

To obtain specific binding affinities for the different chaperones and to underline differences in the binding behaviors, dynamic spectral measurements were carried out during molecular adsorption. A large number of spectra after a certain time interval were recorded during incubation time, then time dependences of Ψ and Δ at a selected wavelength near the plasmon resonance were extracted (see Fig. S1 in the Supporting Material). Because the parameter of Δ has a 10-times better signal/noise ratio than Ψ, the time dependences of Δ are selected for the analysis of binding kinetics.

The procedure of such analysis, described in detail earlier (1,5,7,32), is briefly outlined below. The time constant τ was evaluated from $\Delta(t)$ curves by fitting it to the equation $\Delta = a\exp(-t/\tau) + b$. Then the parameter of $1/\tau = k_aC + k_d$ was plotted as a function of the concentration (C) of analyte molecules yielding the rates of adsorption (k_a) and desorption (k_d) as a gradient and intercept of the above linear dependence, respectively. The association constant K_A of the receptor-chaperone interaction can therefore be described as $KA = k_a/k_d$.

Typical graphs $1/\tau = k_aC + k_d$ for binding of Hsp70-1 at low and high concentrations, respectively, are illustrated in Fig. 5. A rising linear dependence at low concentrations of chaperone (Fig. 5 *A*) results in an affinity constant K_A of $(1.03 \pm 0.18) \times 10^9$ l/mol (Table 2), indicating a highly

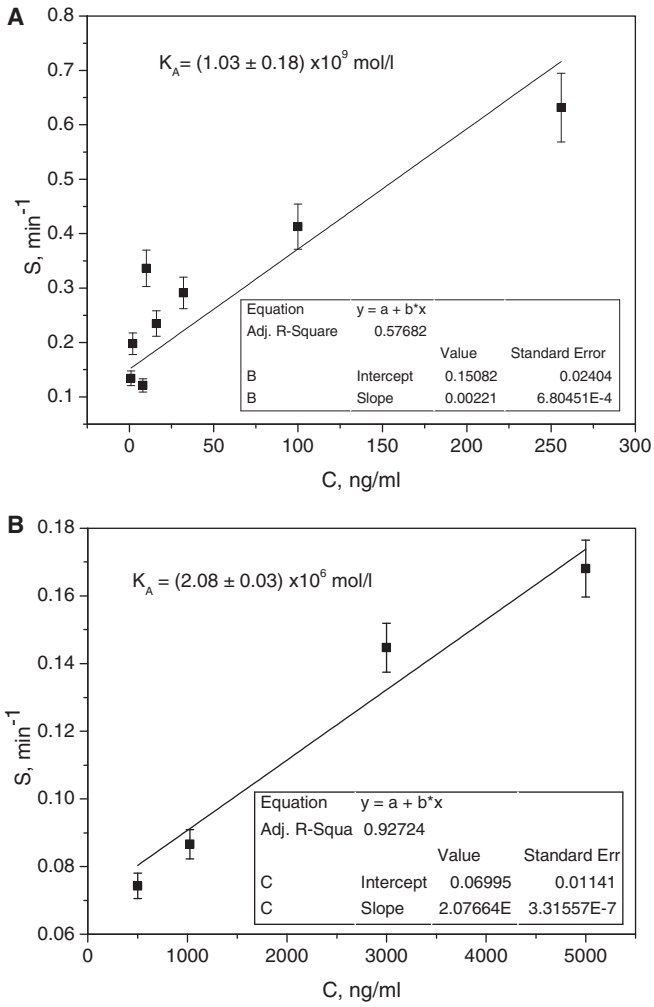

FIGURE 5 Calculations for Hsp70-1 binding affinities to OEP61 at low (*A*) and high (*B*) chaperone concentrations.

TABLE 2 Affinity constant for different receptors and chaperones

		K_A (l/mol)	
Receptor	Chaperone	Low concentration	High concentration
OEP61	Hsp70-1	$(1.03 \pm 0.18) \times 10^9$	$(2.08 \pm 0.03) \times 10^6$
	Hsp70-2	$(4.00 \pm 0.44) \times 10^8$	$(9.60 \pm 1.43) \times 10^4$
	Hsp70b	$(3.60 \pm 0.70) \times 10^8$	$(1.10 \pm 0.91) \times 10^5$
	Hsp90-2	Not detected	$(9.47 \pm 1.27) \times 10^4$
Hop2A	Hsp90-2	$(4.93 \pm 0.54) \times 10^8$	$(2.46 \pm 0.43) \times 10^4$
Toc64	Hsp90-2	$(7.56 \pm 1.86) \times 10^8$	$(8.34 \pm 0.95) \times 10^5$

specific interaction. At high chaperone concentrations above 1 μg/ml (Fig. 5 *B*), the dependence yields much smaller values of K_A in the range of 10^5 l/mol, which can be attributed to nonspecific binding of the chaperones. Such differences in the adsorption kinetics at lower and higher chaperone concentrations were observed for all receptor/chaperone pairs studied (Table 2). Fitting of kinetic curves (see Fig. S1) and subsequent evaluation of time constants results in an accuracy for kinetics analysis of ~20%. Such accuracy is, however, sufficient to compare binding constants for different Hsp70 isoforms and to distinguish between specific and nonspecific binding as three orders-of-magnitude difference in the affinity constants demonstrate a clear mathematical separation between specific binding at low concentrations and the nonspecific one at higher concentrations.

In these dynamic measurements Hsp70-1 displays a binding affinity of $(1.03 \pm 0.18) \times 10^9$ l/mol (Table 2). This is roughly 2.5-times better binding than for Hsp70-2 and Hsp70b (Table 2) and consistent with binding at lower concentrations in the steady-state experiments (Fig. 2). This might indicate that Hsp70-1 has a generally better TPR domain binding.

Again, no specific binding could be measured between the Hsp90-2 isoform and OEP61, whereas both Hop2A and Toc64 control showed strong binding with similar binding affinities of $(4.93 \pm 0.54) \times 10^8$ l/mol and $(7.56 \pm 1.86) \times 10^8$ l/mol, respectively, proving the used chaperone proteins to be capable of binding.

Chaperones in protein targeting

The molecular chaperones Hsp70 and Hsp90 have been widely implicated in protein targeting to mitochondria and chloroplasts, and receptors capable of recognizing these chaperones have been identified at the surface of both these organelles (19). The chaperone isoforms chosen for these experiments are all cytosolic, so they can potentially be involved in targeting proteins translated in the cytosol to various organelles.

The differences in binding behavior for Hsp70 isoforms in steady state as well as dynamic TIRE measurements are intriguing, as these Hsp70 isoforms share a high amino-acid identity (81–94%) and the C-terminal TPR binding motif PKIEEVD necessary for receptor binding is conserved in all isoforms (see Fig. S2). However, amino-acid variability in the isoforms is higher in the C-terminal amino acids before the motif than for the rest of the protein (see Fig. S2); the amino-acid identity for Hsp70-1 and Hsp70b is only 40% compared to 82% for the overall protein sequence. This indicates that these regions might be responsible for variations in the binding affinities.

The cytosolic chaperone Hsp70-1 shares 94% amino-acid identity with Hsp70-2 and 82% with Hsp70b, but stands out by its ability to bind at the lowest concentrations and possession of the highest binding affinity. Hsp70-1 is ubiquitously present in all plant tissues with slightly elevated levels in leaves (33), and despite being further induced by heat or cold shocks it is constitutively expressed, making it available for protein targeting. Hsp70-1 was previously shown to prevent mistargeting of a nuclear envelope protein in plants (34). In contrast, other Hsp70 isoforms seem to play roles that are more specific: Hsp70-2 is also expressed in all tissues, but only after heat or cold induction. Hsp70b is only present after heat induction, and at lower levels than other Hsp70 isoforms (33), making them both unlikely candidates for general protein targeting roles.

Biologically very interesting is the finding that the two plastidial chaperone receptors OEP61 and Toc64 bind one chaperone type via their TPR domain for protein targeting Hsp70 or Hsp90, respectively (27,13). Although both are involved in protein targeting to the chloroplast, this suggests defined parallel functions for both receptors that could influence targeting specificity and/or efficiency.

CONCLUSIONS

The use of total internal reflection ellipsometry for the study of the interaction of chaperones with their receptors provided what we believe to be new quantitative data and has proven to be sensitive enough to distinguish binding differences, even in the highly related Hsp70 chaperone family. The following was established:

1. The interaction between Hsp70 chaperones and the plastidial chaperone receptor OEP61 is highly specific and similar to the binding between Hsp70 isoforms and the Hsp70-binding domain of Hop (Hop1).
2. Few differences in the amino-acid sequence of Hsp70 isoforms seem to lead to changes in their binding affinity to the OEP61 receptor proteins.
3. A clear separation into specific and nonspecific interaction between chaperones and receptors was observed in both the TIRE sensor response and the affinity constants.
4. The theory of molecular adsorption to single binding sites was proved to be suitable for highly specific interactions between receptors immobilized on the surface and low concentrations of chaperone in solution; it allows the evaluation of critical concentrations of chaperone,

outlining the border between specific and nonspecific interaction. The theory of single adsorption sites may not be applicable for nonspecific interactions of proteins which may occur simultaneously at a number of points.

SUPPORTING MATERIAL

Two figures are available at http://www.biophysj.org/biophysj/supplemental/S0006-3495(11)00708-9.

The authors thank Dr. Jason Young (McGill University, Montreal, Quebec, Canada) and The *Arabidopsis* Information Resource (Stanford, CA) for supplying plasmids.

This work was supported by Engineering for Life research grant No. EP/H000275/1 from the Engineering and Physical Sciences Research Council, Feasibility Study grant No. EP/I016473/1, and a Biotechnology and Biological Sciences Research Council research grant awarded to B.M.A. (No. BB/E01559X/1).

REFERENCES

1. Nabok, A., and A. Tsargorodskaya. 2008. The method of total internal reflection ellipsometry for thin film characterization and sensing. *Thin Solid Films.* 516:8993–9001.
2. Mustafa, M. K., A. Nabok, …, A. Tsargorodskaya. 2010. Detection of β-amyloid peptide (1–16) and amyloid precursor protein (APP770) using spectroscopic ellipsometry and QCM techniques: a step forward towards Alzheimers disease diagnostics. *Biosens. Bioelectron.* 26: 1332–1336.
3. Nabok, A., A. Tsargorodskaya, …, P. J. Higson. 2007. The study of DNA hybridization using total internal reflection ellipsometry. *Biosens. Bioelectr.* 23:377–383.
4. Nabok, A. V., A. Tsargorodskaya, …, N. F. Starodub. 2005. Total internal reflection ellipsometry and SPR detection of low molecular weight environmental toxins. *Appl. Surf. Sci.* 246:381–386.
5. Nabok, A. V., A. Tsargorodskaya, …, O. Gojster. 2007. Registration of T-2 mycotoxin with total internal reflection ellipsometry and QCM impedance methods. *Biosens. Bioelectron.* 22:885–890.
6. Nabok, A., A. Tsargorodskaya, …, A. Szekacs. 2010. Detection of low molecular weight toxins using optical phase detection techniques. *Sens. Actuators B Chem.* 154:232–237.
7. Nabok, A. V., A. Tsargorodskaya, …, A. Demchenko. 2007. Specific binding of large aggregates of amphiphilic molecules to the respective antibodies. *Langmuir.* 23:8485–8490.
8. Arwin, H., M. Poksinski, and K. Johansen. 2004. Total internal reflection ellipsometry: principles and applications. *Appl. Opt.* 43: 3028–3036.
9. Lvov, Y., and H. Mohwald. 2000. Protein architecture. *In* Interfacing Molecular Assemblies and Immobilization Biotechnology.. Marcel Dekker, New York 167.
10. Nabok, A. V., S. Haron, and A. K. Ray. 2004. Optical enzyme sensors based upon silicon planar waveguide coated with composite polyelectrolyte film. *Appl. Surf. Sci.* 238:423–428.
11. Starodub, N. F., A. V. Nabok, …, A. K. Hassan. 2001. Immobilization of biocomponents for immune optical sensors. *Ukr. Biochem. J.* 73: 55–64.
12. Wickner, W., and R. Schekman. 2005. Protein translocation across biological membranes. *Science.* 310:1452–1456.
13. Qbadou, S., T. Becker, …, E. Schleiff. 2006. The molecular chaperone Hsp90 delivers precursor proteins to the chloroplast import receptor Toc64. *EMBO J.* 25:1836–1847.
14. Chew, O., R. Lister, …, J. Whelan. 2004. A plant outer mitochondrial membrane protein with high amino acid sequence identity to a chloroplast protein import receptor. *FEBS Lett.* 557:109–114.
15. Brinker, A., C. Scheufler, …, F. U. Hartl. 2002. Ligand discrimination by TPR domains. Relevance and selectivity of EEVD-recognition in Hsp70 × Hop × Hsp90 complexes. *J. Biol. Chem.* 277:19265–19275.
16. Scheufler, C., A. Brinker, …, I. Moarefi. 2000. Structure of TPR domain-peptide complexes: critical elements in the assembly of the Hsp70-Hsp90 multichaperone machine. *Cell.* 101:199–210.
17. Wu, S. J., F. H. Liu, …, C. Wang. 2001. Different combinations of the heat-shock cognate protein 70 (Hsc70) C-terminal functional groups are utilized to interact with distinct tetratricopeptide repeat-containing proteins. *Biochem. J.* 359:419–426.
18. Odunuga, O. O., J. A. Hornby, …, G. L. Blatch. 2003. Tetratricopeptide repeat motif-mediated Hsc70-mSTI1 interaction. Molecular characterization of the critical contacts for successful binding and specificity. *J. Biol. Chem.* 278:6896–6904.
19. Schlegel, T., O. Mirus, …, E. Schleiff. 2007. The tetratricopeptide repeats of receptors involved in protein translocation across membranes. *Mol. Biol. Evol.* 24:2763–2774.
20. Kriechbaumer, V., O. von Löffelholz, and B. M. Abell. 2011. Chaperone receptors: guiding proteins to intracellular compartments. *Protoplasma.*, in press.
21. Abell, B. M., C. Rabu, …, S. High. 2007. Post-translational integration of tail-anchored proteins is facilitated by defined molecular chaperones. *J. Cell Sci.* 120:1743.
22. Artigues, A., A. Iriarte, and M. Martinez-Carrion. 2002. Binding to chaperones allows import of a purified mitochondrial precursor into mitochondria. *J. Biol. Chem.* 277:25047–25055.
23. Lin, B.-L., J.-S. Wang, …, M. Delseny. 2001. Genomic analysis of the Hsp70 superfamily in *Arabidopsis thaliana*. *Cell Stress Chaperones.* 6:201–208.
24. Wu, C. H., T. Caspar, …, C. Somerville. 1988. Characterization of an HSP70 cognate gene family in *Arabidopsis*. *Plant Physiol.* 88: 731–740.
25. Wu, S. H., C. Wang, …, B. L. Lin. 1994. Isolation of a cDNA encoding a 70 kDa heat-shock cognate protein expressed in vegetative tissues of *Arabidopsis thaliana*. *Plant Mol. Biol.* 25:577–583.
26. Sangster, T. A., and C. Queitsch. 2005. The HSP90 chaperone complex, an emerging force in plant development and phenotypic plasticity. *Curr. Opin. Plant Biol.* 8:86–92.
27. v. Loeffelholz, O., V. Kriechbaumer, …, B. M. Abell. 2011. OEP61 is a chaperone receptor at the plastid outer envelope. *Biochem. J.* 10.1042/BJ20110448 Epub ahead of print.
28. Young, J. C., N. J. Hoogenraad, and F. U. Hartl. 2003. Molecular chaperones Hsp90 and Hsp70 deliver preproteins to the mitochondrial import receptor Tom70. *Cell.* 112:41–50.
29. Woollam, J. A. 2002. Guide to Using WVASE32. J.A. Woollam Company, Lincoln, NE.
30. Székács, A., N. Adányi, …, I. Szendrő. 2009. Optical waveguide lightmode spectroscopy immunosensors for environmental monitoring. *Appl. Opt.* 48:151–158.
31. Chen, S., and D. F. Smith. 1998. Hop as an adaptor in the heat shock protein 70 (Hsp70) and Hsp90 chaperone machinery. *J. Biol. Chem.* 273:35194–35200.
32. Liu, X., J. Wei, …, G. Luo. 2003. Determination of affinities and antigenic epitopes of bovine cardiac troponin I (cTnI) with monoclonal antibodies by surface plasmon resonance biosensor. *Anal. Biochem.* 314:301–309.
33. Sung, D. Y., E. Vierling, and C. L. Guy. 2001. Comprehensive expression profile analysis of the *Arabidopsis* Hsp70 gene family. *Plant Physiol.* 126:789–800.
34. Brkljacic, J., Q. Zhao, and I. Meier. 2009. WPP-domain proteins mimic the activity of the HSC70-1 chaperone in preventing mistargeting of RanGAP1-anchoring protein WIT1. *Plant Physiol.* 151:142–154.